

Article

Preparation of Antiproliferative Terpene-Alkaloid Hybrids by Free Radical-Mediated Modification of *ent*-Kauranic Derivatives

Elena Pruteanu ^{1,2}, Vladilena Gîrbu ¹, Nicon Ungur ¹, Leentje Persoons ³, Dirk Daelemans ³, Philippe Renaud ^{2,*} and Veaceslav Kulcički ^{1,*}

- ¹ Institute of Chemistry (MECC), Str. Academiei, 3, MD-2028 Chişinău, Moldova; elena.pruteanu@unibe.ch (E.P.); vgirbu1@gmail.com (V.G.); nicon.ungur@gmail.com (N.U.)
² Department of Chemistry, Biochemistry and Pharmaceutical Sciences, University of Bern, Freiestrasse 3, 3012 Bern, Switzerland
³ KU Leuven, Department of Microbiology, Immunology and Transplantation, Laboratory of Virology and Chemotherapy, Rega Institute for Medical Research, Herestraat 49, 3000 Leuven, Belgium; leentje.persoons@rega.kuleuven.be (L.P.); dirk.daelemans@kuleuven.be (D.D.)
* Correspondence: philippe.renaud@unibe.ch (P.R.); kulcitki@yahoo.com (V.K.)

Abstract: A convenient strategy for molecular editing of available *ent*-kauranic natural scaffolds has been developed based on radical mediated C–C bond formation. Iodine atom transfer radical addition (ATRA) followed by rapid ionic elimination and radical azidoalkylation were investigated. Both reactions involve radical addition to the *exo*-methylene double bond of the parent substrate. Easy transformations of the obtained adducts lead to extended diterpenes of broad structural diversity and artificial diterpene-alkaloid hybrids possessing lactam and pyrrolidine pharmacophores. The cytotoxicity of selected diterpenic derivatives was examined by in vitro testing on several tumor cell lines. The terpene-alkaloid hybrids containing *N*-heterocycles with unprecedented spiro-junction have shown relevant cytotoxicity and promising selectivity indexes. These results represent a solid basis for following research on the synthesis of such derivatives based on available natural product templates.

Keywords: diterpene; *ent*-kaurane; alkaloids; radical chemistry; ATRA; lactam; lactone; spiro compound; azide; pyrrolidine; cytotoxicity



Citation: Pruteanu, E.; Gîrbu, V.; Ungur, N.; Persoons, L.; Daelemans, D.; Renaud, P.; Kulcički, V. Preparation of Antiproliferative Terpene-Alkaloid Hybrids by Free Radical-Mediated Modification of *ent*-Kauranic Derivatives. *Molecules* **2021**, *26*, 4549. <https://doi.org/10.3390/molecules26154549>

Academic Editor: Maria José U. Ferreira

Received: 21 June 2021

Accepted: 19 July 2021

Published: 28 July 2021

Publisher's Note: MDPI stays neutral with regard to jurisdictional claims in published maps and institutional affiliations.



Copyright: © 2021 by the authors. Licensee MDPI, Basel, Switzerland. This article is an open access article distributed under the terms and conditions of the Creative Commons Attribution (CC BY) license (<https://creativecommons.org/licenses/by/4.0/>).

1. Introduction

The kauranic family of diterpenes is widespread in diverse plant sources and some representatives are readily available for large scale processing. The best known examples are *ent*-kaurenoic acid **1** and steviol **2** (Figure 1), which can be conveniently isolated from industrial crop derived products or residues. *Iso*-steviol **3** can also be included in this group, since it easily forms upon acidic hydrolysis of steviol **2** glycosides found in the *Stevia Rebaudiana* plant and is broadly used as an alternative non-caloric sweetener [1]. These compounds alone possess relevant biological activities [2–4], and numerous SAR studies have been reported based on their structural modifications [5–7]. In particular, chemical modification of steviol **2** and especially *iso*-steviol **3** has been well explored and delivered diverse compound libraries, basing on chemical reactivity of both carboxylic groups, as well as D-cycle functionalities [6,7].

ent-kaurenoic acid **1** has also been extensively involved in SAR studies and chemical modification was reported frequently at the level of the carboxylic functional group. The reactivity of the *exo*-methylene Δ^{16} -double bond was mostly addressed via the heteroatom addition processes or trivial oxidative transformations and only scarce data involve deeper skeletal modifications based on this functionality [8,9]. The *exo*-methylene moiety of acid **1** represents an additional opportunity for increasing molecular complexity based upon

free radical processes. Free radical transformations are mild and versatile molecular editing tools, which have gained increasing popularity within the natural product chemistry community due to their tremendous potential for convenient late-stage functionalization of natural product scaffolds. Remote C–H functionalization is one example [10–12]. As a logical consequence, medicinal chemistry research can fully benefit from the structural diversity generated by free radical transformations of available natural product templates.

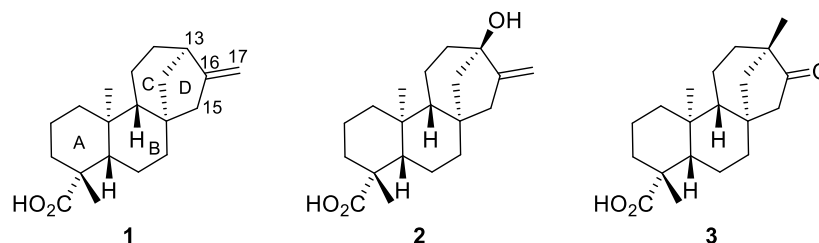
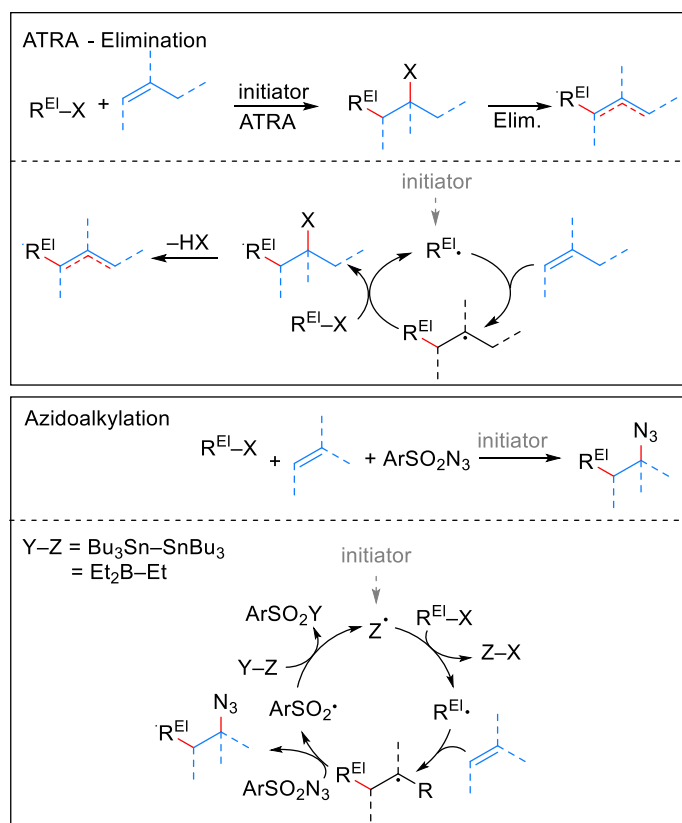


Figure 1. Structures of *ent*-kaurenoic acid **1**, steviol **2** and *iso*-steviol **3**.

In this context, we turned our attention to two mild free radical processes that proved efficient for the functionalization of olefinic bonds in other compound families: the atom transfer radical addition (ATRA) and the azidoalkylation reaction. ATRA are highly attractive transformations originating from the work of Kharasch, who discovered the addition of activated alkyl halides to alkenes [13–15]. This pioneering work was further refined into a valuable synthetic procedure [16] with a positive impact in diverse areas of chemistry [17]. Briefly, ATRA involves a starting alkyl halide with a weak C–X bond, which upon homolytic cleavage generates a carbon-centered radical prone to interaction with the olefinic moiety of the substrate in an addition process (Scheme 1, top). The resulting free radical abstracts the X-atom from the alkyl halide and the reaction chain perpetuates. Iodine-ATRA reactions leading to tertiary iodides are often followed by a rapid elimination of HI and conversion to alkenes [18,19]. The azidoalkylation reaction is closely related to the ATRA process but involves an extra azidating agent, usually a sulfonyl azide (Scheme 1, bottom) [20–22]. This reaction has been applied for the synthesis of several alkaloids [22–24] and its stereochemistry has been investigated in detail [25]. The formal result of both transformations is a carbo-functionalization of the alkene, including the simultaneous formation of both C–C and C–heteroatom bonds.

Such transformations are quite efficient and can be run under very mild reaction conditions, compatible with other functional groups present in the substrate. Therefore, it represents an ideal tool for molecular editing within SAR studies of complex molecules like *ent*-kauranes. It is worth mentioning that the *exo*-methylenic double bond in *ent*-kauranes is regarded as one of the crucial elements in the interaction with molecular targets [5] and the structural modifications of the diterpene skeleton at the level of C (16)–C (17) carbon atoms can result in new properties of the corresponding derivatives. In this respect, C (17) alkylated *ent*-kauranes have been sporadically isolated from natural sources. A recent example relates to helikaurolicides A (**4**) and B (**5**) (Figure 2)—unprecedented *ent*-kauranes, prenylated at C (17) with a densely functionalized sesquiterpene unit [26]. Biogenetically, both **4** and **5** have been hypothesized based upon *ent*-kaurenoic acid **1** alkylation with the sesquiterpene unit. Therefore, radical C (17) alkylations represent an exact mimic of this biogenetical mechanism. Having this in mind, we report in the current paper the results of the synthesis and cytotoxic activity of new *ent*-kauranes based on radical additions to the *exo*-methylenic double bond of *ent*-kaurenoic acid **1** and its derivatives.



Scheme 1. Mild transformation of alkenes via ATRA (-elimination) and azidoalkylation: useful tools for molecular editing (R^{El} = electrophilic C-residue).

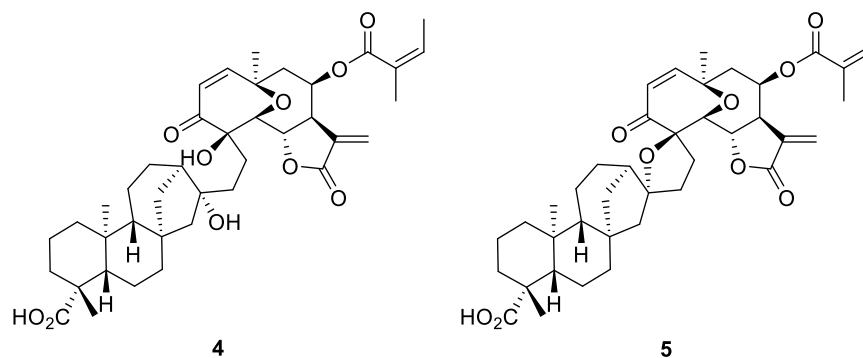


Figure 2. Structures of helikaurolides A (4) and B (5).

2. Results and Discussions

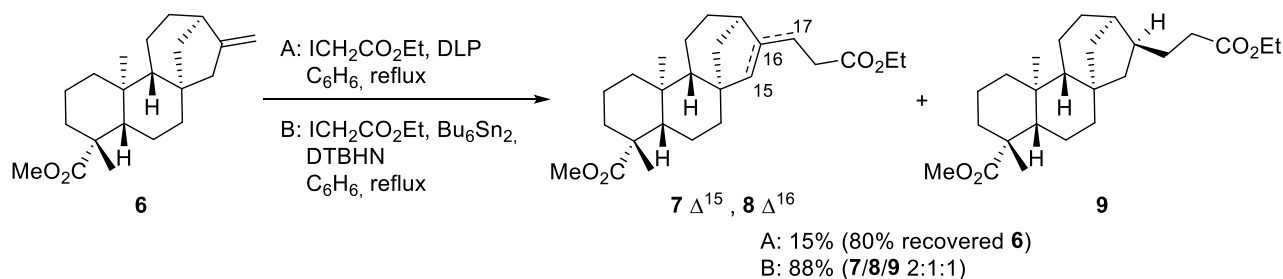
2.1. Radical Addition to *ent*-Kaurenoates

2.1.1. Iodine-ATRA Reactions

Carboiodination is a process that formally adds an alkyl group and an iodine atom to the olefinic moieties. It is the simplest version of ATRA, and we started our work with carboiodination of methyl *ent*-kaurenoate **6**. It was prepared upon methylation of acid **1** with diazomethane. Ethyl iodoacetate was chosen as a readily available alkylating agent. The reaction was performed in refluxing benzene under inert atmosphere in the presence of dilauroyl peroxide (DLP) as an initiator (Scheme 2, Method A) [27].

DLP was gradually added to the reaction mixture in portions of 0.05 equivalents every 2 h during 24 h of reflux. Under these conditions, the conversion was sluggish and the starting ester **6** was recovered unchanged, along with minor amounts of esters **7–9** (15%). Their formation can be explained by the instability of the initially formed tertiary iodide, which eliminates HI to provide **7** and **8**. A hydrogen atom transfer, possibly involving

DLP, can explain the formation of saturated **9**. The separation of these compounds was difficult and only the endocyclic isomer **7** was isolated in a sufficiently pure form to provide satisfactory spectral data.



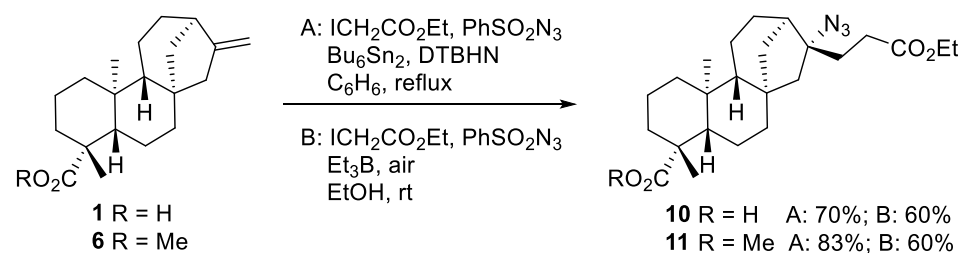
Scheme 2. Iodine-ATRA of ethyl iodoacetate to methyl-*ent*-kaurenoate **6**.

In order to increase the conversion rate, we performed the reaction under the action of a hexabutylditin–*di-tert*-butyl hyponitrite (DTBHN) system, which showed good results in similar transformations [28]. The reaction resulted in the almost complete consumption of the starting material over 2 h at reflux and a mixture of esters **7–9** was produced with an 88% yield (Scheme 2, Method B, **7/8/9** 2:1:1). The formation of the tertiary iodide was not observed. Such eliminations of tertiary iodides has been described in the literature [18].

2.1.2. Azidoalkylation

At this stage, it became clear that an efficient regiocontrol over HI elimination represents quite a challenging task for substrates with *exo*-methylenic double bonds. Therefore, we turned our attention to the azidoalkylation reaction, a transformation of special value from a SAR perspective due to the broad opportunities offered by the azide group for further transformation [29] such as 1,3-dipolar cycloaddition (click reaction) [30] and reduction to primary amines.

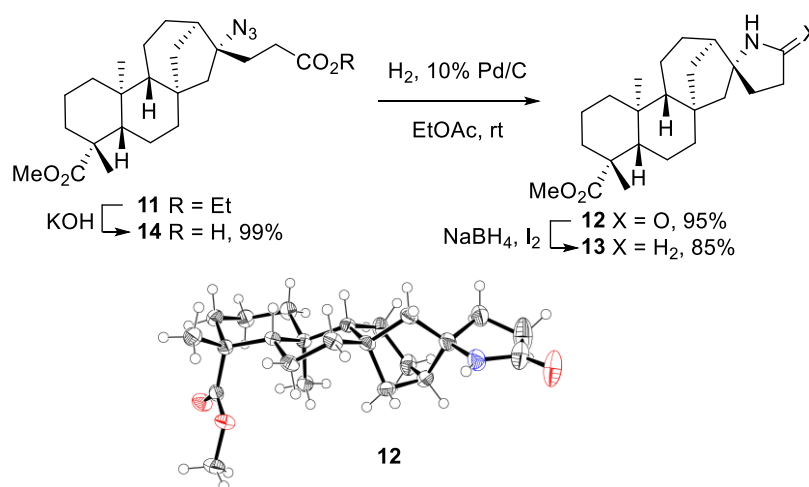
Azidoalkylation of acid **1** was performed under standard conditions using ethyl iodoacetate (radical precursor) and phenylsulfonyl azide (azidating agent) in the presence of hexabutylditin (chain transfer reagent) and DTBHN as an initiator [20]. The reaction proceeded well and the resulting azide **10** was isolated in 70% yield (Scheme 3, Method A). The free carboxyl group remained intact. Unfortunately, the purification of the product was difficult and total removal of residual tin contaminants was not possible. In order to avoid this problem, we investigated azidoalkylation of the corresponding methyl ester **6** under the same conditions. The azide **11** was isolated with an 83% yield without noticeable contamination by tin residues. To avoid the use of toxic hexabutylditin, the reaction was attempted using triethylborane as a mediator [31,32]. The compatibility of triethylborane with the free carboxylic functional group of **1** was expected to be an issue [33,34]. We decided to circumvent this problem by using a two-fold excess of Et₃B and aqueous workup to hydrolyze acyloxyboron derivatives. The addition products **10** and **11** were both isolated in satisfactory 60% yields (Scheme 3, Method B).



Scheme 3. Azidoalkylation of *ent*-kaurenoic acid **1** and methyl-*ent*-kaurenoate **6**.

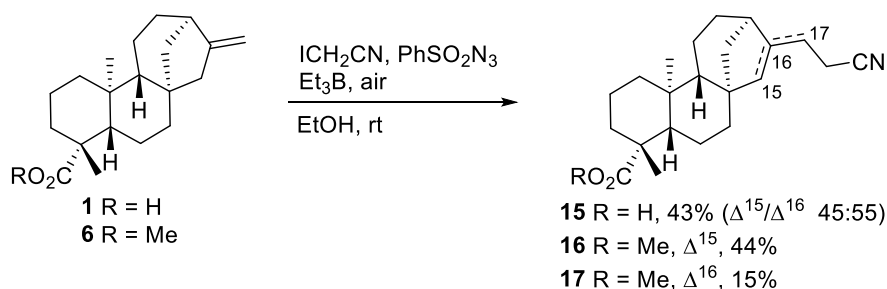
To prepare the terpene-alkaloid hybrids, the product γ -azidoester **11** was converted to *N*-containing heterocycles. The hydrogenation of azide **11** went smoothly under 1 atmo-

sphere of hydrogen pressure and Pd/C as a catalyst. The initially formed primary amine spontaneously formed the lactam **12** during the reduction (Scheme 4). Further reduction of the lactam **12** with NaBH₄/I₂ furnished the pyrrolidine **13** [35]. The spiro-cyclic system in both **12** and **13** represents a novel *ent*-kauranic-alkaloid hybrid that turned out to be a relevant pharmacophore, as revealed by cytotoxicity testing experiments described below. The relative stereochemistry of lactam **12** has been determined by single crystal X-ray crystallography (Scheme 4) [36]. These data confirmed indirectly the relative stereochemistry of starting azide **11**, showing that the addition of azide radicals occurred in a highly stereoselective way from the less hindered convex face of the tetracyclic *ent*-kauranic framework [25]. Furthermore, the ethyl ester moiety of azide **11** could be selectively hydrolyzed to provide the azido acid **14** in nearly quantitative yield.



Scheme 4. Conversion of the azidoalkylated product **11** into lactam **12**, pyrrolidine **13** and azido acid **14**. X-ray crystal structure of lactam **12** (ellipsoids drawn at 50% probability, CCDC 2023783).

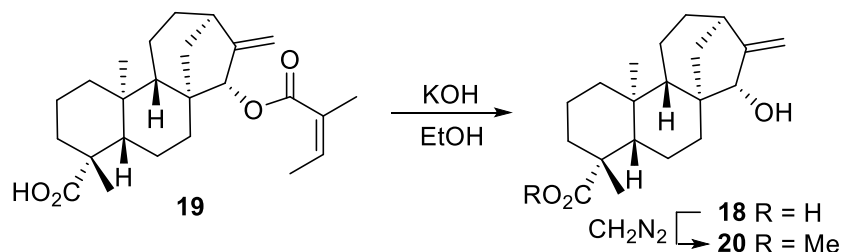
We also observed that the nature of the iodide represents an important factor affecting azidoalkylation of acid **1** and ester **6**. Our attempt to use iodoacetonitrile instead of ethyl iodoacetate did not result in any azidoalkylated product under Et₃B initiation. The major reaction products are the unsaturated nitriles **15–17** (Scheme 5), similar in structure to esters **7** and **8**. This result is presumably due to the formation of an unstable iodide intermediate in the case of the nitrile, while the ester radical adduct reacts directly with the sulfonyl azide without the formation of a transient iodide. Indeed, iodoacetonitrile is a better iodine atom donor than the corresponding ester by about two orders of magnitude [37]. Trace amounts of an azide obtained from the azidoalkylation of acid **1** have been tentatively identified based on the characteristic ¹³C NMR peak at 72.25 ppm, corresponding to the C-N₃ carbon atom. The isolation of this minor product turned out to be impossible using standard chromatography techniques.



Scheme 5. Azidoalkylation attempt of methyl-*ent*-kaurenoate **6** with iodoacetonitrile.

2.2. Radical Addition to 15 α -Hydroxy-*ent*-Kaurenoates

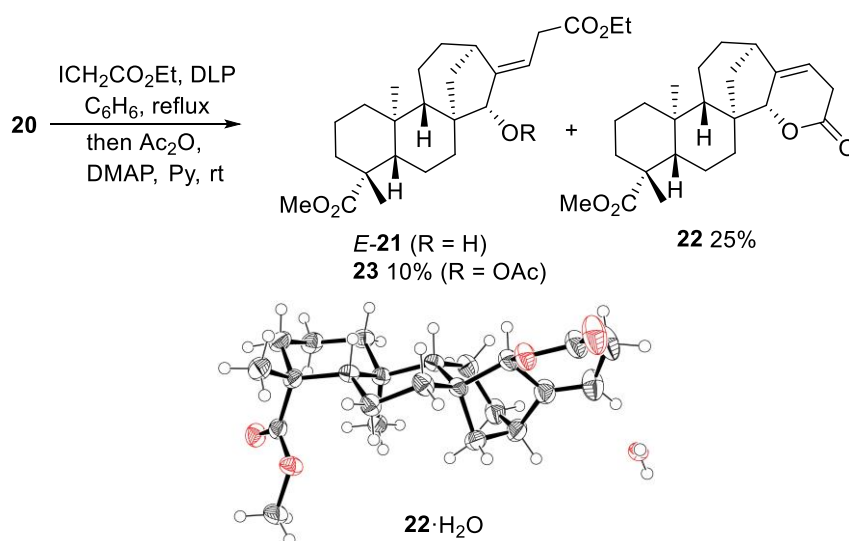
The modification of methyl 15 α -hydroxy-*ent*-kaurenoate **20** was investigated next. The hydroxylated *ent*-kauranic acid derivative **18** comes together with *ent*-kaurenoic acid **1** in the sunflower vegetal mass as an angelic acid ester **19**. The latter can be easily isolated and hydrolyzed to provide pure **18** (Scheme 6). Methylation of **18** with diazomethane furnished quantitatively the methyl ester **20** used for the radical mediated modification experiments.



Scheme 6. Preparation of methyl 15 α -hydroxy-*ent*-kaurenoate **20**.

2.2.1. Iodine ATRA Reactions

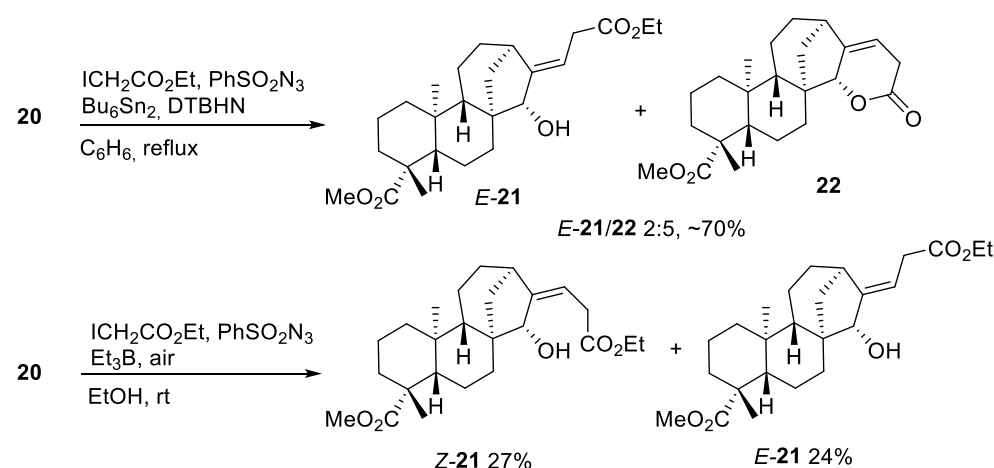
Upon heating the ester **20** with ethyl iodoacetate in benzene under DLP initiation, a mixture of two major unsaturated compounds *E*-**21** and **22** was obtained (Scheme 6). In line with similar ATRA experiments with substrates **1** and **6**, the hypothetically formed tertiary iodide is unstable, and rapid HI elimination leads to the unsaturated products [18]. Due to the presence of the alcohol moiety in **20**, lactonization of the *Z*-alkene resulting from the ATRA-elimination process occurred spontaneously under these reaction conditions leading to the unsaturated lactone **22**. The *E*-alkene cannot cyclize and the ester *E*-**21** is formed. Chromatographic separation of *E*-**21** from lactone **22** proved to be difficult due to their similar retention factors. Acetylation of the mixture of **21** and **22** with acetic anhydride resulted in the formation of acetate **23** which could be easily separated by chromatography and provided satisfactory analytical data for full characterization (Scheme 7). The structure of lactone **22** was obtained by single crystal X-ray crystallography (Scheme 7) [36]. The basic challenge at this stage was the demonstration of the *E*-configuration of the exocyclic double bond in acetate **23** and indirectly in alcohol **21**. The convincing proof came from the experiments on azidoalkylation of the allylic alcohol **20** (see below).



Scheme 7. Addition of ethyl iodoacetate to **20**. X-ray crystal structure of lactone **22**·H₂O (ellipsoids drawn at 50% probability, CCDC 2023785).

2.2.2. Azidoalkylation

The azidoalkylation process was investigated under similar conditions that brought about optimal conversion of methyl *ent*-kaurenoate **6** to the azide **11**. Upon treatment of **20** with ethyl iodoacetate in the presence of hexabutyltin–DTBHN and phenylsulfonyl azide, an optimal 90% conversion of starting material was achieved after 5 h of heating at reflux in benzene (Scheme 8). However, no azide was detected but the already known ester *E*-**21** and lactone **22** were obtained. When the same reaction was run at room temperature under triethylborane initiation, again no azide was formed, and a mixture of unsaturated esters *E*-**21** and *Z*-**21** was obtained (Scheme 8). Interestingly, the lower reaction temperature impedes the lactonization of *Z*-**21** and its isolation was possible. The absence of the azidoalkylated product is presumably a consequence of the increased steric hindrance and decreased nucleophilicity of the hydroxylated radical adduct relative to the non-hydroxylated one, leading to **11**.



Scheme 8. Iodine-ATRA between methyl 15 α -hydroxy-*ent*-kaurenoate **20** and ethyl iodoacetate.

Having accessed all four compounds *E*-**21**, *Z*-**21**, **22**, and **23** of sufficient purity, we were able to draw conclusions on their stereochemistry based on the ^1H NMR spectra, in particular upon examining the splitting character of C (18) methylenic protons adjacent to the carboxylic group in these compounds (Figure 3).

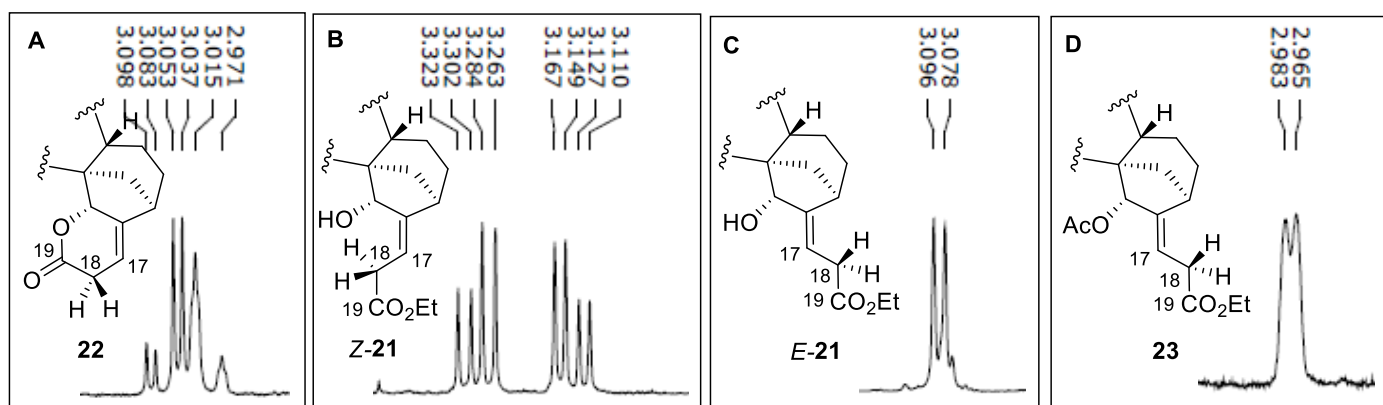
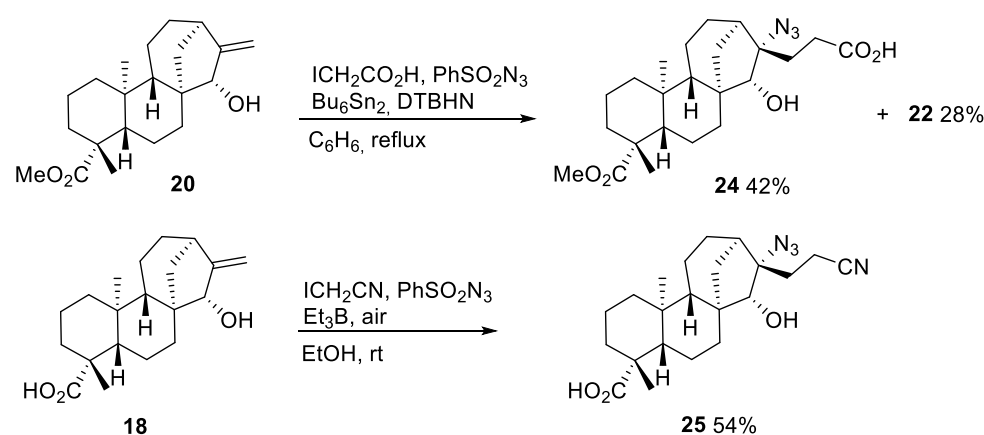


Figure 3. ^1H NMR spectra sections of lactone **21** (A), ester **24** (B), ester **22** (C), and acetate **23** (D).

First, these methylenic protons in **22** resonate at 3.02 ppm (Figure 3A) and show a relevant geminal coupling, which is due to the rigid cyclic structure and strong influence of the adjacent oxygenated moieties. The vicinal coupling with the vinylic proton is in accordance with dihedral angles observed in X-ray pictures. The ^1H NMR spectrum of *Z*-**21** shows a similar splitting profile of the methylenic group at C (18) (Figure 3B, 3.11–3.32 ppm)

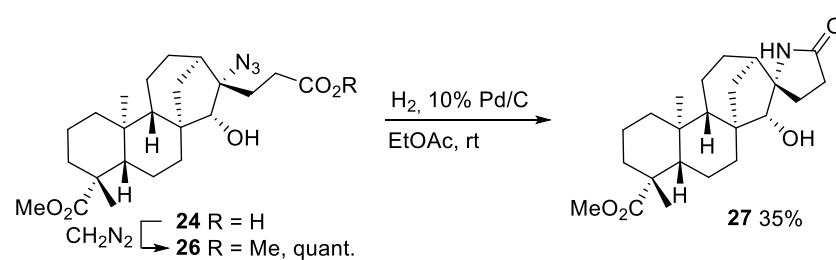
to that observed in lactone **22**, demonstrating the proximity of this group to the hydroxyl at C (15) position, leading to a larger chemical shift difference between two geminal protons at C (18). On the other hand, both C (18) methylenic protons in ester *E*-**21** and acetate **23** are almost equivalent due to the conformational mobility of the lateral chain and impeded interaction with the oxygenated functional group. Their NMR peaks represent doublets, resonating at 3.08 ppm (Figure 3C) and 2.97 ppm (Figure 3D), respectively, and having an identical coupling constant of 7.3 Hz with vinylic protons from C (17).

Interestingly, an attempt to run the azidoalkylation process with iodoacetic acid instead of its ethyl ester led to the azide **24** and lactone **22** (Scheme 9). The azidoalkylation was also achieved with iodoacetonitrile as the radical precursor. Performing the reaction with triethylborane as radical initiator was compatible with the free carboxyl group in the starting *ent*-kaurane **18** and resulted in product **25**, opening up more opportunities for further functionalization.



Scheme 9. Azidoalkylation of methyl 15- α -hydroxy-*ent*-kauranoate **20** and 15- α -hydroxy-*ent*-kauranoic acid **18** with iodoacetic acid and iodoacetonitrile.

Further transformations of azido-acid **24** included its methylation with diazomethane to ester **26**, which could be converted into lactam **27** during reduction of the azide under hydrogenation conditions (Scheme 10).



Scheme 10. Conversion of the azidoalkylated acid **24** into ester **26** and lactam **27**.

2.3. Cytotoxicity Testing

The described processes resulted in a small library of new compounds with modified *ent*-kaurane skeletons, and their cytotoxic activity has been investigated. Proliferation assays have been performed in seven different tumor cell lines as shown in Table 1: Capan-1 (pancreatic adenocarcinoma), HCT-116 (colorectal carcinoma), NCI-H460 (lung carcinoma), DND-41 (acute lymphoblastic leukemia), HL-60 (acute myeloid leukemia), K-562 (chronic myeloid leukemia), and Z-138 (non-Hodgkin lymphoma). A parallel cytotoxicity assay was performed on non-cancerous retina cells (hTERT RPE-1) in order to estimate the selectivity of the investigated compounds towards tumor cells. The inhibition of cell proliferation was calculated as IC₅₀ by interpolation based on the semi-log dose response. Docetaxel and staurosporine have been included as positive controls. The data in Table 1 show that a significant

portion of the investigated compounds demonstrate relevant antitumoral activity. In particular, compounds **11–13**, **22**, **26**, and **27** were active with IC₅₀ values below 1 μM concentrations. We were also pleased to observe a selective activity for some compounds, based on much higher IC₅₀ for normal non-cancerous cells. The calculated selectivity indices (SI), i.e., the ratio of the IC₅₀ for normal cells to the IC₅₀ for the corresponding tumor cells [38], are higher than the threshold value of 3 for several samples (see table in the supplementary material for details). The highest selectivity indices were obtained for compounds **11**, **12**, **13**, **26**, and **27**, with IC₅₀ values for retina (hTERT RPE-1) cells up to 43-fold higher than those for cancerous cells. These data are indicative of a potential therapeutic index for these compounds, which can be explored in subsequent in vivo toxicity tests.

Table 1. Antiproliferative activity of *ent*-kauranic derivatives. DT—docetaxel; SP—staurosporine.

Compound	Conc. Unit	IC ₅₀							
		hTERT RPE-1	Capan-1	HCT-116	NCI-H460	DND-41	HL-60	K-562	Z-138
7	μM	29.2 ± 1.2	37.1 ± 3.9	30.7 ± 16.4	12.0 ± 1.5	36.5 ± 0.7	19.6 ± 7.7	24.7 ± 11.8	27.6 ± 15.5
11	μM	1.8 ± 0.4	1.7 ± 0.5	1.0 ± 0.4	1.3 ± 0.1	1.4 ± 0.3	3.0 ± 1.4	8.8 ± 2.2	0.5 ± 0.2
12	μM	7.6 ± 0.5	1.2 ± 0.7	0.8 ± 0.2	1.4 ± 0.1	21.4 ± 10.1	38.3 ± 17.8	36.4 ± 11.5	52.0 ± 33.4
13	μM	32.2 ± 2.0	11.5 ± 1.0	11.6 ± 0.5	1.0 ± 0.1	6.1 ± 1.1	8.3 ± 1.3	3.2 ± 1.0	9.5 ± 0.9
14	μM	26.2 ± 0.9	44.5 ± 8.3	5.8 ± 0.1	31.1 ± 1.6	44.5 ± 4.8	46.2 ± 9.1	41.0	22.7
16	μM	38.2 ± 5.1	18.1 ± 3.4	19.0 ± 5.7	15.4 ± 6.0	7.8 ± 1.0	33.6 ± 2.6	58.4 ± 2.5	22.1 ± 11.4
22	μM	1.4 ± 0.1	1.3 ± 0.6	0.5 ± 0.2	1.4 ± 0.3	2.3 ± 0.3	3.7 ± 1.3	2.5 ± 0.1	2.4 ± 1.1
24	μM	31.7 ± 3.1	33.2 ± 7.6	18.8 ± 8.0	41.8 ± 5.3	38.9 ± 4.1	49.3 ± 5.0	76.3 ± 1.4	25.2 ± 0.3
25	μM	33.6 ± 4.5	6.4 ± 1.5	34.4 ± 0.5	34.0 ± 2.9	36.4 ± 9.8	>100	>100	52.0 ± 17.4
26	μM	25.9 ± 0.3	8.3 ± 1.1	9.9 ± 2.7	0.6 ± 0.2	6.6 ± 1.3	41.1 ± 15.9	36.9 ± 0.2	21.6 ± 5.4
27	μM	27.7 ± 4.3	3.7 ± 1.7	4.0 ± 3.7	1.9 ± 0.2	8.3 ± 2.0	38.0 ± 11.8	56.5 ± 2.8	39.8 ± 10.9
DT	nM	18.7 ± 4.8	4.2 ± 1.8	2.2 ± 0.8	5.5 ± 1.3	4.7 ± 1.2	4.3 ± 1.6	5.2 ± 1.2	3.7 ± 0.7
SP	nM	1.0	6.2 ± 1.8	1.5	2.2 ± 0.8	8.6 ± 1.5	9.1 ± 1.6	27.9 ± 3.2	6.7 ± 4.4

From a structural topology point of view, the most active compounds show some relevant similarities (Figure 4). First of all, most of the active compounds include nitrogen containing functional groups. The second structural convergence relates to the cyclic backbone, which includes an extra cycle to the natural *ent*-kauranic framework. Exceptions are azides **11** and **26**. Finally, three of the four most relevant cytotoxic compounds with high selectivity towards tumor cells are heterocycles **12**, **13**, and **27** with a spirocyclic fragment. To the best of our knowledge, such derivatives of *ent*-kauranic compounds have never been reported in SAR studies. The activity levels of these compounds is much higher than that of the reference drug Cisplatin (IC₅₀ 16.5 for HCT-116 and 5.33 for NCI-H460) and in the same range as the currently marketed drug midostaurine, with IC₅₀ 0.237 for HCT-116 and 0.43 for NCI-H460 [39]. In fact, compounds **12** and **27** share the same γ-lactam unit with both natural staurosporine and synthetic midostaurine. Although this pharmacophore is becoming increasingly more studied [40], little is known about the properties of γ-spiro-1-lactams, which are extremely rare in the literature. The same relates to their mechanism of interaction with cellular targets [41]. Following in vivo toxicity studies can reveal the therapeutic potential of the reported new *ent*-kauranic derivatives.

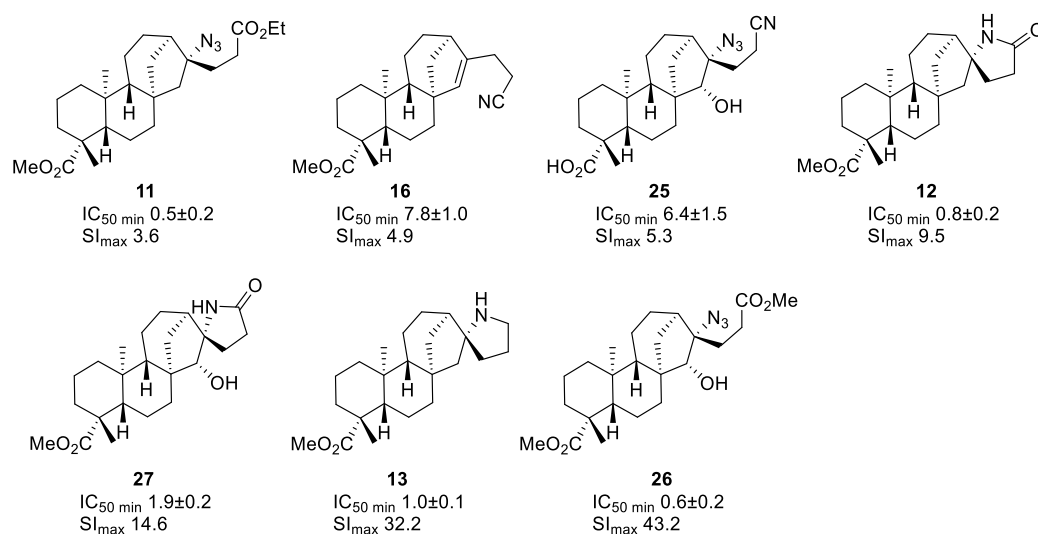


Figure 4. Relevant cytotoxic activity parameters for selected compounds.

3. Materials and Methods

3.1. Chemistry General Section

IR spectra were recorded on a Perkin–Elmer (Beaconsfield, UK) Spectrum 100 FT-IR spectrophotometer using the universal ATR sampling accessory. NMR spectra were recorded in $CDCl_3$ on a Bruker (Rheinstetten, Germany) Avance III spectrometer (400.13 and 100.61 MHz). Chemical shifts (δ) are reported in parts per million (ppm) downfield from tetramethylsilane $Si(CH_3)_4$ ($\delta = 0.00$ for 1H NMR spectra) using residual solvent signal as an internal standard: δ singlet 7.26 (1H), triplet 77.0 (^{13}C) for $CDCl_3$ or δ singlet 4.87 (1H), septet 49.0 (^{13}C) for CD_3OD . Multiplicities are given as s (singlet), d (doublet), t (triplet), q (quadruplet), m (multiplet), and bs (broad signal). Coupling constant (J) is reported in Hz. In case of mix of products, selected values for 1H NMR were reported (as specified in the description). In ^{13}C NMR spectra, the peak positions are reported to one decimal unless the difference in chemical shift between two signals (for example for regio-/diastereoisomers) is small and required two decimals. Optical rotations were measured in $CHCl_3$ or MeOH on a Jasco DIP 370 polarimeter, using a 5-cm cell. GC-MS experiments were performed on an Agilent 7890A (Wilmington, DE, USA) chromatograph equipped with a quadrupole MS detector MSD 5975C and an HP-5ms capillary column (30 m/0.25 mm/0.25 μm). Analytical TLC was performed on Fluka Silica Alu foils. Usual workup included dilution with brine and extraction with Et_2O . The organic phases have been dried over Na_2SO_4 , filtered and the solvent evaporated under reduced pressure to provide the crude reaction product. Column chromatography (CC) was performed with Fluka Kieselgel 60 silica gel. All solvents were of reagent grade and other reagents have been used as received from suppliers. DLP was added in aliquot portions every 2 h to the solution of the corresponding olefin and iodide. Addition of Et_3B solutions (commercial) to the reaction mixtures was performed via a syringe with the needle immersed into the reaction mixture to avoid direct contact of Et_3B drops with air. ATRA reactions have been performed with ethyl iodoacetate unless otherwise specified. Benzene and THF have been dried according to standard procedures and distilled before use.

3.2. Crystal-Structure Determination

The crystals were mounted in air at ambient conditions. All measurements were made on an Oxford Diffraction SuperNova area-detector diffractometer [42] using mirror optics monochromated Mo $K\alpha$ radiation ($\lambda = 0.71073 \text{ \AA}$) and Al filtered [43]. Data reduction was performed using the *CrysAlisPro* [42] program. The intensities were corrected for Lorentz and polarization effects, and an absorption correction based on the multi-scan method using SCALE3 ABSPACK in *CrysAlisPro* [42] was applied. Data collection, refinement

parameters and other specific experimental details are given in the Supplementary Materials. The structure was solved by direct methods using *SHELXT* [44], which revealed the positions of all non-hydrogen atoms of the title compound. The non-hydrogen atoms were refined anisotropically. All H-atoms were placed in geometrically calculated positions and refined using a riding model where each H-atom was assigned a fixed isotropic displacement parameter with a value equal to 1.2U_{eq} of its parent atom. Refinement of the structure was carried out on F^2 using full-matrix least-squares procedures, which minimized the function $\sum w (F_o^2 - F_c^2)^2$. The weighting scheme was based on counting statistics and included a factor to downweight the intense reflections. All calculations were performed using the *SHELXL-2014/7* [45] program in *OLEX2* [46].

3.3. Cytotoxicity Testing

3.3.1. Cell Culture and Reference Compounds

All cell lines (HL-60, K-562, Z-138, Capan-1, HCT-116, NCI-H460 and hTERT RPE-1) were acquired from the American Type Culture Collection (ATCC, Manassas, VA, USA), except for the DND-41 cell line, which was purchased from the Deutsche Sammlung von Mikroorganismen und Zellkulturen (DSMZ Leibniz-Institut, Braunschweig, Germany). All cell lines were cultured as recommended by the suppliers. Culture media were purchased from Gibco Life Technologies, USA, and supplemented with 10% fetal bovine serum (HyClone, GE Healthcare Life Sciences, Logan, UT, USA). Reference inhibitor compounds staurosporine and docetaxel were obtained from Selleckchem (Munich, Germany). All stock solutions were prepared in DMSO.

3.3.2. Cell Proliferation Assays

Adherent cell lines Capan-1, HCT-116 and NCI-H460 cells were seeded at a density between 500 and 1500 cells per well in 384-well clear-bottomed tissue culture plates (Greiner). After overnight incubation, cells were treated with the test compounds at seven different concentrations ranging from 100 to 6.4×10^{-3} μ M. Suspension cell lines DND-41, HL-60, K-562, and Z-138 were seeded at densities ranging from 2500 to 5500 cells per well in 384-well clear-bottomed tissue culture plates containing the test compounds at the same seven concentration points. The plates were incubated at 37 °C and monitored for 72 h in an IncuCyte[®] device (Essen BioScience Inc., Ann Arbor, MI, USA) for real-time imaging. Images were taken every 3 h, with one field imaged per well under 10 \times magnification. Cell growth was then quantified based on the percent cellular confluence as analysed by the IncuCyte[®] image analysis software and used to calculate IC₅₀ values by linear interpolation. All tests have been performed in duplicate and the average values have been calculated. The corresponding mean values and deviations are provided in Table 1.

3.4. Experimental Section

DLP-mediated ATRA to methyl *ent*-kaurenoate

Methyl *ent*-kaurenoate **6** (50 mg, 0.16 mmol) in dry C₆H₆ (5 mL) was treated with ethyl iodoacetate (28 μ L, 0.24 mmol) and DLP (3 mg, 0.008 mmol). The reaction mixture was heated on reflux under N₂ for 24 h. The mixture was purified by CC (hexane/EtOAc 98:2) and gave unchanged starting material (40 mg, 80%) and a mixture of compounds **7**, **8** and **9** (10 mg, 15%).

Ester **7**

Pale yellow viscous oil. $[\alpha]_D^{20} = -45.8$ ($c = 8.13$, CHCl₃). IR (ν , cm⁻¹): 3804, 3736, 3674, 3608, 2927, 1728, 1445, 1231, 1156. ¹H NMR (400 MHz, CDCl₃) δ_H : 5.07 (s, 1H, CH-15), 4.13 (q, $J = 7.1$ Hz, 2H, -CO₂CH₂CH₃), 3.63 (s, 3H, -CO₂CH₃), 2.44–2.49 (m, 2H, -CH₂-COOEt), 1.25 (t, $J = 7.1$ Hz, 3H, -CO₂CH₂CH₃), 1.16 (s, 3H, CH₃-20), 0.83 (s, 3H, CH₃-22), 2.38–0.93 (m, 21H). ¹³C NMR (100 MHz, CDCl₃) δ_C : 178.0, 173.4, 145.1, 134.4, 60.2, 56.9, 51.0, 49.0, 47.8, 43.9, 43.8, 40.8, 39.6, 39.5, 38.2, 32.4, 29.7, 28.7, 25.4, 25.3, 20.8, 19.2, 18.9, 15.2, 14.2. GCMS m/z calculated for [C₂₅H₃₈O₄]⁺: 402.28; found: 402.3.

Ester 8

Mixture of 2 diastereomers. IR (ν , cm^{-1}): 3674, 2931, 1728, 1449, 1234, 1171, 1150. ^1H NMR (400 MHz, CDCl_3) selected values, δ_{H} : 4.15–4.09 (m, 2H, $-\text{CO}_2\text{CH}_2\text{CH}_3$), 3.64 (s, 3H, $-\text{CO}_2\text{CH}_3$), 1.25 (m, 3H, $-\text{CO}_2\text{CH}_2\text{CH}_3$), 1.17 (m, 3H, CH_3 -20), 0.82 (m, 3H, CH_3 -22). ^{13}C NMR (100 MHz, CDCl_3) selected values, δ_{C} : 178.04/178.03, 172.57/172.41, 149.98/148.94, 110.39/109.94, 60.36, 57.12/57.07, 55.17/55.10, 51.03, 49.32/46.21, 43.84, 43.59/43.48, 41.41/41.19, 40.80, 39.63/39.47, 39.41/39.27, 38.12, 34.90/34.68, 33.06/30.83, 28.73, 21.96, 19.16, 18.76/18.45, 15.45/15.41, 14.21/14.18. GCMS m/z calculated for $\text{C}_{25}\text{H}_{38}\text{O}_4$: 402.28; found: 402.3.

Ester 9

Colorless oil. IR (ν , cm^{-1}): 3750, 2921, 1729, 1506, 1448, 1370, 1191, 1042. ^1H NMR (400 MHz, CDCl_3) δ_{H} : 4.12 (q, $J = 7.9$ Hz, 2H, $-\text{CO}_2\text{CH}_2\text{CH}_3$), 3.63 (s, 3H, $-\text{CO}_2\text{CH}_3$), 2.86–2.60 (m, 1H), 2.29 (m, 2H, CH_2 -17), 1.25 (t, $J = 7.1$ Hz, 3H, $-\text{CO}_2\text{CH}_2\text{CH}_3$), 1.16 (s, 3H, CH_3 -20), 0.81 (s, 3H, CH_3 -22), 2.18–0.79 (m, 23H). ^{13}C NMR (100 MHz, CDCl_3) δ_{C} : 178.10, 174.03, 60.17, 57.15, 56.61, 51.05, 46.74, 44.41, 43.89, 42.22, 40.87, 40.51, 40.13, 39.48, 38.49, 38.21, 34.09, 28.77, 26.66, 25.88, 22.24, 19.19, 19.14, 15.42, 14.28. GCMS m/z calculated for $\text{C}_{25}\text{H}_{40}\text{O}_4$: 404.29; found: 404.3.

Bu_6Sn_2 -mediated ATRA to methyl *ent*-kaurenoate

Methyl *ent*-kaurenoate **6** (50 mg, 0.158 mmol) in dry C_6H_6 (3 mL) was treated under N_2 with ethyl iodoacetate (37.4 μL , 0.316 mmol), Bu_6Sn_2 (120 μL , 0.237 mmol), and DTBHN (0.8 mg, 0.005 mmol). The reaction mixture was refluxed for 2 h. The crude product was purified by CC (hexane/EtOAc 98:2) and gave a 2:1:1 mixture of compounds **7**, **8**, and **9** (61 mg, 88% total yield). Separation of this mixture on a silver nitrate impregnated silica afforded a pure sample of ester **7** (45% yield), along with esters **8** and **9** (22% and 21% yield, respectively).

Bu_6Sn_2 -mediated ATRA to *ent*-kaurenoic acid

ent-Kaurenoic acid **1** (87 mg, 0.29 mmol) in dry benzene (2 mL) was treated under N_2 with ethyl iodoacetate (51.5 μL , 0.44 mmol), PhSO_2N_3 (159 mg, 0.87 mmol), Bu_6Sn_2 (222 μL , 0.44 mmol), and DTBHN (1.5 mg, 0.087 mmol). The reaction mixture was refluxed for 2 h and after this time the crude product was purified by CC (pentane/EtOAc 90:10) giving compound **10**, slightly contaminated with tin compounds (NMR). This impurified product was methylated with an ethereal solution of diazomethane and purified by CC (hexane/EtOAc 98:2) to afford azide **11** (90 mg, 70%) as a colorless oil.

Azide 11

Colorless viscous oil. $[\alpha]_{\text{D}}^{20} = -79.5$ ($c = 0.84$, CHCl_3). IR (ν , cm^{-1}): 2944, 2873, 2096, 1727, 1502. ^1H NMR (400 MHz, CDCl_3) δ_{H} : 4.12 (q, $J = 7.2$ Hz, 2H, $-\text{CO}_2\text{CH}_2\text{CH}_3$), 3.62 (s, 3H, $-\text{CO}_2\text{CH}_3$), 2.42 (t, $J = 7.9$ Hz, 2H, $-\text{CH}_2-\text{COOEt}$), 1.25 (t, $J = 7.2$ Hz, 3H, $-\text{CO}_2\text{CH}_2\text{CH}_3$), 1.14 (s, 3H, CH_3 -20), 0.80 (s, 3H, CH_3 -22), 2.06–0.75 (m, 23H). ^{13}C NMR (100 MHz, CDCl_3) δ_{C} : 177.9, 173.4, 73.1, 60.5, 56.7, 55.8, 51.5, 51.1, 44.7, 44.3, 43.7, 41.4, 40.6, 39.4, 38.0, 37.7, 30.3, 29.7, 28.7, 26.1, 22.0, 19.0, 18.5, 15.3, 14.2. GCMS m/z calculated for $[\text{C}_{25}\text{H}_{39}\text{N}_3\text{O}_4]$: 445.28; found: 402.3 ($\text{M}-\text{HN}_3$).

Bu_6Sn_2 -mediated ATRA to methyl *ent*-kaurenoate

Methyl *ent*-kaurenoate **6** (100 mg, 0.36 mmol) in dry benzene (2 mL) was treated under N_2 with ethyl iodoacetate (64 μL , 0.54 mmol), PhSO_2N_3 (200 mg, 1.08 mmol), Bu_6Sn_2 (272 μL , 0.54 mmol), and DTBHN (2 mg, 0.01 mmol). The reaction mixture was refluxed for 2 h. The crude product was purified by column chromatography (hexane/EtOAc 98:2) and gave the azide **11** (133 mg, 83%).

Et_3B -mediated ATRA to *ent*-kaurenoic acid

ent-Kaurenoic acid **1** (44 mg, 0.146 mmol) in dry EtOH (2 mL) was treated under N₂ with ethyl iodoacetate (35 μ L, 0.292 mmol), PhSO₂N₃ (80 mg, 0.438 mmol), Et₃B (0.6 mL, 0.584 mmol). The reaction was stirred at room temperature overnight then diluted with brine and worked up. The crude product was purified by CC (hexane/EtOAc 94:6) giving pure compound **10** (39 mg, 60%).

Azide **10**

Pale yellow viscous oil. $[\alpha]_D^{20} = -69.2$ (c = 1.9, CHCl₃). IR (ν , cm⁻¹): 2935, 2900, 2872, 2848, 2626, 2098, 1734, 1693. ¹H NMR (400 MHz, CDCl₃) δ (ppm) 4.14 (q, *J* = 7.1 Hz, 2H, -CO₂CH₂CH₃), 2.43 (t, *J* = 8.1 Hz, 2H, -CH₂-COOEt), 1.26 (t, *J* = 7.1 Hz, 3H, -CO₂CH₂CH₃), 1.22 (s, 3H, CH₃-20), 0.93 (s, 3H, CH₃-22), 2.15–0.73 (m, 23H). ¹³C NMR (100 MHz, CDCl₃) δ (ppm) 184.9, 173.4, 73.1, 60.6, 56.7, 55.8, 51.5, 44.7, 44.3, 43.7, 41.4, 40.5, 39.6, 37.7, 37.6, 30.3, 29.7, 28.9, 26.1, 21.8, 18.9, 18.5, 15.4, 14.2.

Et₃B-mediated ATRA to methyl *ent*-kaurenoate

Methyl *ent*-kaurenoate **6** (50 mg, 0.16 mmol) in dry EtOH (2 mL) was treated under N₂ with ethyl iodoacetate (39 μ L, 0.33 mmol), PhSO₂N₃ (87 mg, 0.47 mmol) and Et₃B (0.47 mL). The reaction mixture was stirred for 2 h at room temperature. The crude product was purified by column chromatography (pentane/EtOAc 98:2) and gave the azide **11** (43 mg, 60%).

Lactam **12**

A solution of azide **11** (53 mg, 0.12 mmol) and 10% Pd/C (10% *w/w*) in dry EtOAc (2 mL) was stirred for 48 h at room temperature under H₂ (1 atm). The catalyst was filtered off, the solvent was removed under reduced pressure, and the crude purified by column chromatography (CH₂Cl₂/MeOH 90:10) giving lactam **12** (42 mg, 95%) as a white powder.

White powder. M.p. 150–152 °C, from CH₂Cl₂. $[\alpha]_D^{20} = -77.4$ (c = 4.50, CHCl₃). IR (ν , cm⁻¹): 3676, 3209, 2937, 2298, 1712, 1683. ¹H NMR (400 MHz, CDCl₃) δ_H : 6.68 (s, 1H, -NH), 3.63 (s, 3H, -CO₂CH₃), 2.30 (m, 2H, CH₂-17), 2.05 (d, *J* = 11.9 Hz, 2H, CH₂-18), 1.15 (s, 3H, CH₃-20), 0.81 (s, 3H, CH₃-22), 2.36–0.79 (m, 21H). ¹³C NMR (100 MHz, CDCl₃) δ_C : 177.9, 176.8, 67.2, 57.6, 56.9, 55.6, 51.1, 46.6, 44.9, 43.8, 41.8, 40.7, 39.4, 38.9, 38.1, 31.1, 30.0, 28.7, 27.1, 22.0, 19.1, 18.8, 15.4.

Pyrrolidine **13**

To a solution of lactam **12** (50 mg, 0.13 mmol) in THF (4 mL) were added NaBH₄ (20 mg, 0.53 mmol) and I₂ (102 mg, 0.4 mmol). The reaction mixture was refluxed for 8 h, then cooled at 0 °C and excess hydride quenched with 3N HCl solution, then neutralized and worked up as usual. The crude product was purified by CC (CH₂Cl₂/MeOH 90:10) giving compound **13** (40 mg, 85%) as a colorless oil.

Colorless oil. $[\alpha]_D^{20} = -73.6$ (c = 2.74, CHCl₃). IR (ν , cm⁻¹): 3424, 2940, 2871, 2744, 2483, 1722, 1599. ¹H NMR (400 MHz, CDCl₃) δ (ppm) 8.46 (s, 1H, NH) 3.63 (s, 3H, -CO₂CH₃), 3.43 (bs, 2H, CH₂-19), 2.65 (s, 1H, CH-13), 1.15 (s, 3H, CH₃-20), 0.81 (s, 3H, CH₃-22), 2.09–0.78 (m, 24H). ¹³C NMR (100 MHz, CDCl₃) δ (ppm) 177.9, 76.8, 56.7, 55.7, 52.4, 51.1, 45.7, 43.8, 43.3, 42.7, 40.7, 40.3, 39.5, 38.5, 38.1, 33.0, 28.6, 26.9, 22.7, 22.1, 19.0, 18.6, 15.3.

Azide **14**

Azide **11** (50 mg, 0.11 mmol) was dissolved in EtOH and treated with KOH (31.4 mg, 0.56 mmol) on reflux for 2 h. Then, the reaction mixture was diluted with brine and extracted with Et₂O and ethereal extract washed with 10% sol. H₂SO₄, sat. sol. NaHCO₃, brine and dried over Na₂SO₄. The crude product was purified by CC (petroleum ether/EtOAc 90:10), providing the azide **14** as colorless oil (45 mg, 98%).

Colorless oil. $[\alpha]_D^{20} = -85.6$ (c = 4.50, CHCl₃). IR (ν , cm⁻¹): 3855, 3668, 2942, 2098, 1724, 1715, 1446, 1236, 1154, 1066, 1051, 774. ¹H NMR (400 MHz, CDCl₃) δ_H : 3.64 (s, 3H, -CO₂CH₃), 2.51 (t, *J* = 7.97 Hz, 2H, CH₂-17), 1.16 (s, 3H, CH₃-20), 0.82 (s, 3H, CH₃-22), 2.16–0.99 (m, 23H). ¹³C NMR (100 MHz, CDCl₃) δ_C : 178.6, 178.0, 72.9, 56.7, 55.8, 51.5, 51.2, 44.8, 44.3, 43.7, 41.4, 40.6, 39.4, 38.0, 37.7, 29.9, 29.5, 28.7, 26.2, 22.0, 19.0, 18.5, 15.3.

Et₃B-mediated ATRA of iodoacetonitrile to *ent*-kaurenoic acid.

ent-Kaurenoic acid **1** (190.0 mg, 0.63 mmol) in 3.5 mL EtOH was treated under N₂ with iodoacetonitrile (91 μ L, 1.25 mmol), PhSO₂N₃ (345.0 mg, 1.88 mmol) and Et₃B (1.9 mL, 1.88 mmol) at room temperature overnight. The crude product was purified by FC (petroleum ether/EtOAc 90:10) and provided the isomeric mixture **15** (95 mg, 42%, Δ^{15} : Δ^{16} = 45:55, NMR data).

Mixture of nitriles **15**

IR (ν , cm⁻¹): 3671, 2923, 2854, 2666, 1696, 1469, 1445, 1413. ¹H NMR (400 MHz, CDCl₃) selected values, δ_{H} : 5.23 (s, CH-15), 5.18–5.14 (m, CH-17), 2.98 (s, 2xCH₂-18), 2.15 (m, CH₂-17 Δ^{15}), 1.24, 1.23 (s, CH₃-20), 0.93, 0.95 (s, CH₃-22); ¹³C NMR (100 MHz, CDCl₃) selected values, δ_{C} (major Δ^{16}): 184.04, 153.35, 118.38, 105.82, 56.99, 54.94, 45.94, 44.02, 41.20, 40.67, 39.67, 39.30, 37.75, 32.87, 28.92, 21.79, 19.05, 18.41, 17.04, 15.59; (minor Δ^{15}): 184.26, 142.85, 136.04, 119.73, 56.72, 49.22, 47.42, 43.76, 43.40, 40.66, 39.85, 39.26, 37.79, 28.94, 25.96, 25.32, 20.67, 19.05, 18.95, 15.56, 15.38.

Et₃B-mediated ATRA of iodoacetonitrile to methyl *ent*-kaurenoate

Methyl *ent*-kaurenoate **6** (180.0 mg, 0.56 mmol) in 3.5 mL EtOH was treated under N₂ with iodoacetonitrile (82 μ L, 1.13 mmol), PySO₂N₃ (313.0 mg, 1.7 mmol), and Et₃B (1.7 mL, 1.7 mmol) at room temperature overnight. The crude product was purified by CC (petroleum ether/EtOAc 95:5) and provided the mixture of unsaturated derivatives **16** and **17** (117 mg, 58%, **16**/**17** = 3:1, NMR data). This mixture was submitted to a repetitive separation on a silver nitrate impregnated silica column and individual nitriles slightly contaminated with a second isomer were obtained as a colorless oils.

Nitrile **16**

Colorless oil. $[\alpha]_{\text{D}}^{20}$ = -48.8 (c = 4.6, CHCl₃). IR (ν , cm⁻¹): 2932, 2848, 1723, 1639, 1468, 1446, 1232, 1158. ¹H NMR (400 MHz, CDCl₃) δ_{H} : 5.22 (s, 1H, CH-15), 3.63 (s, 3H, -CO₂CH₃), 2.49–2.38 (m, 2H, CH₂-18), 1.15 (s, 3H, CH₃-20), 0.99 (s, 3H, CH₃-22), 2.19–0.78 (m, 21H). ¹³C NMR (100 MHz, CDCl₃) δ_{C} : 178.0, 142.8, 136.0, 119.8, 56.7, 51.1, 49.2, 47.4, 43.8, 43.8, 43.4, 40.7, 39.6, 39.3, 38.1, 28.7, 25.9, 25.3, 20.7, 19.1, 18.9, 15.5, 15.2.

Nitrile **17**

Colorless oil. $[\alpha]_{\text{D}}^{20}$ = -100.8 (c = 3.4, CHCl₃). IR (ν , cm⁻¹): 2931, 2855, 1723, 1461, 1447, 1150. ¹H NMR (400 MHz, CDCl₃) δ_{H} : 5.17–5.13 (m, 1H, CH-17), 3.64 (s, 3H, -CO₂CH₃), 3.04 (m, 2H, CH₂-18), 2.84 (bs, 1H), 2.21–1.96 (m, 1H), 1.17 (s, 3H, CH₃-20), 0.83 (s, 3H, CH₃-22), 2.06–0.79 (m, 19H). ¹³C NMR (100 MHz, CDCl₃) δ_{C} : 178.1, 152.5, 118.9, 106.5, 57.2, 55.1, 51.3, 49.3, 44.0, 43.8, 41.2, 40.9, 39.7, 39.6, 38.2, 30.8, 29.7, 28.9, 22.1, 19.3, 18.9, 17.2, 15.7.

DLP-mediated ATRA to methyl 15 α -hydroxy-*ent*-kaurenoate

Methyl 15 α -hydroxy-*ent*-kaurenoate **20** (56 mg, 0.17 mmol) in 3.7 mL benzene was treated under N₂ with ethyl iodoacetate (60 μ L, 0.507 mmol) and DLP (3.4 mg, 0.009 mmol). The reaction was refluxed for 24 h and after this time the crude product was purified by FC (pentane/EtOAc 95:5), giving a mixture of lactone **22** and ester *E*-**21** (25 mg, **22**/*E*-**21** = 5:2 ratio, NMR data). This mixture was acetylated with acetic anhydride (0.2 mL, 2.6 mmol) and DMAP (0.5 mol%) in pyridine (5 mL) at room temperature for 48 h. The crude mixture was extracted with Et₂O, neutralized with 10% aqueous H₂SO₄ and washed with brine. The organic layer was dried, and the solvent was removed under reduced pressure. The crude was purified by column chromatography (pentane/EtOAc 97:3) to afford pure lactone **22** (16 mg, 25%) and acetate **23** (8 mg, 10%).

Lactone **22**

White solid. M.p. 180–182 °C, from CH₂Cl₂. $[\alpha]_{\text{D}}^{20}$ = +11.4 (c = 2.83, CHCl₃). IR (ν , cm⁻¹): 3054, 2986, 2933, 2865, 1740, 1722. ¹H NMR (400 MHz, CDCl₃) δ_{H} : 5.81 (dt, *J* = 5.4, 2.3 Hz, 1H, CH-17), 4.48 (d, *J* = 1.66 Hz, 1H, CH-15), 3.64 (s, 3H, -CO₂CH₃), 3.03 (m, 2H,

CH₂-18), 2.82 (bs, 1H, CH-13), 1.19 (s, 3H, CH₃-20), 0.86 (s, 3H, CH₃-22), 2.20–0.84 (m, 18H). ¹³C NMR (100 MHz, CDCl₃) δ_C: 177.9, 172.6, 148.9, 115.3, 88.0, 56.8, 54.6, 51.1, 46.1, 43.8, 40.8, 40.7, 39.6, 38.4, 38.0, 34.3, 33.1, 30.0, 28.7, 20.7, 19.0, 18.9, 15.7. GCMS *m/z* calculated for C₂₃H₃₂O₄: 359.28; found 328.2 (M⁺ -CO₂).

Ester 23

Colorless oil. [α]_D²⁰ = −69.8 (c = 2.36, CHCl₃). IR (ν, cm^{−1}): 2984, 2930, 2859, 1727. ¹H NMR (400 MHz, CDCl₃) δ_H: 5.62 (t, *J* = 7.4 Hz, 1H, CH-17), 5.44 (s, 1H, CH-15), 4.12 (q, *J* = 7.8, 7.3 Hz, 2H, -CO₂CH₂CH₃), 3.63 (s, 3H, -CO₂CH₃), 2.97 (d, *J* = 7.1 Hz, 2H, CH₂-18), 2.79 (bs, 1H, CH-13), 2.07 (s, 3H, -O (CO)CH₃), 1.25 (t, *J* = 7.9 Hz, 3H, -CO₂CH₂CH₃), 1.15 (s, 3H, CH₃-20), 0.81 (s, 3H, CH₃-22), 2.20–0.80 (m, 18H). ¹³C NMR (100 MHz, CDCl₃) δ_C: 177.9, 171.5, 170.7, 148.7, 117.3, 80.7, 60.6, 56.6, 52.5, 51.1, 47.8, 43.8, 42.3, 40.6, 39.7, 37.9, 37.0, 34.7, 34.3, 33.1, 28.6, 20.9, 20.8, 19.1, 18.4, 15.5, 14.2.

Bu₆Sn₂-mediated ATRA to methyl 15α-hydroxy-*ent*-kaurenoate

Methyl 15α-hydroxy-*ent*-kaurenoate **20** (50 mg, 0.15 mmol) in 3.2 mL benzene was treated under N₂ with ethyl iodoacetate (36 μL, 0.3 mmol), PhSO₂N₃ (83 mg, 0.45 mmol), Bu₆Sn₂ (115 μL, 0.23 mmol) and DTBHN (0.9 mg, 0.005 mmol). The reaction mixture was refluxed for 5 h. The crude product was purified by FC (pentane/EtOAc 95:5) and gave a mixture of compounds **22** and *E*-**21** (43 mg, **22**/*E*-**21** = 5:2, NMR data), along with unreacted starting material (5 mg, 10%).

Et₃B-mediated ATRA to methyl 15α-hydroxy-*ent*-kaurenoate

Methyl 15α-hydroxy-*ent*-kaurenoate **20** (50 mg, 0.15 mmol) in 3.5 mL EtOH was treated under N₂ with ethyl iodoacetate (36 μL, 0.3 mmol), PhSO₂N₃ (83 mg, 0.45 mmol) and Et₃B (0.45 mL, 0.45 mmol) at room temperature overnight. The crude product was purified by column chromatography (pentane/EtOAc 95:5) and afforded unreacted starting material **20** (7 mg, 14%), ester *Z*-**21** (17 mg, 27%, contaminated with cca. 20% *E*-**21**), and pure ester *E*-**21** (15 mg, 24%).

Ester *E*-21

Colorless oil. [α]_D²⁰ = −89.8 (c = 4.80, CHCl₃). IR (ν, cm^{−1}): 3484, 2933, 2871, 1724, 1463, 1447, 1370, 1329, 1233, 1191, 1153. ¹H NMR (400 MHz, CDCl₃) δ_H: 5.80 (t, *J* = 7.3 Hz, 1H, CH-17), 4.13 (q, *J* = 7.1 Hz, 2H, -CO₂CH₂CH₃), 3.77 (s, 1H, CH-15), 3.64 (s, 3H, -CO₂CH₃), 3.09 (d, *J* = 7.5 Hz, 2H, CH₂-COOEt), 1.25 (t, *J* = 7.1 Hz, 3H, -CO₂CH₂CH₃), 1.17 (s, 3H, CH₃-20), 0.83 (s, 3H, CH₃-22) 2.85–0.72 (m, 18H). ¹³C NMR (100 MHz, CDCl₃) δ_C: 178.11, 171.90, 153.54, 116.42, 83.18, 60.69, 56.96, 52.89, 51.16, 47.33, 43.82, 40.75, 39.60, 38.02, 36.09, 35.14, 35.09, 34.65, 30.56, 28.72, 21.03, 19.13, 18.66, 15.64, 14.19.

Ester *Z*-21

Colorless oil. IR (ν, cm^{−1}): 3484, 2932, 2872, 1725, 1464, 1448, 1372, 1312, 1233, 1191, 1155. ¹H NMR (400 MHz, CDCl₃) selected values, δ_H: 5.50 (t, *J* = 7.8 Hz, 1H, CH-17), 4.14 (q, *J* = 7.1 Hz, 2H, -CO₂CH₂CH₃), 3.95 (s, 1H, CH-15), 3.64 (s, 3H, -CO₂CH₃), 3.11–3.32 (m, 2H, CH₂-COOEt), 1.25 (t, *J* = 7.1 Hz, 3H, -CO₂CH₂CH₃), 1.18 (s, 3H, CH₃-20), 0.82 (s, 3H, CH₃-22). ¹³C NMR (100 MHz, CDCl₃) selected values, δ_C: 178.03, 172.79, 154.79, 115.62, 80.40, 60.96, 57.06, 53.11, 51.05, 47.79, 43.84, 42.13, 40.80, 39.61, 38.06, 36.00, 35.12, 33.18, 28.69, 21.07, 19.15, 18.27, 15.57, 14.13.

Bu₆Sn₂-mediated ATRA of iodoacetic acid to methyl 15α-hydroxy-*ent*-kaurenoate

Methyl 15α-hydroxy-*ent*-kaurenoate **20** (64.0 mg, 0.192 mmol) in 2.0 mL benzene was treated under N₂ with iodoacetic acid (71.4 mg, 0.38 mmol), PhSO₂N₃ (105.0 mg, 0.57 mmol), Bu₆Sn₂ (145 μL, 0.28 mmol), and DTBHN (1.0 mg, 0.006 mmol). The reaction mixture was refluxed for 5 h. The crude product was purified by CC (petroleum ether/EtOAc 70:30) to provide lactone **22** (23 mg, 28%) and azide **24** as a colorless oil (91 mg, 42%, contaminated with PhSO₂N₃).

Azide 24

Colorless oil. IR (ν , cm^{-1}): 3675, 2988, 2955, 2928, 2902, 2108, 1724, 1553. ^1H NMR (400 MHz, D_3COD) δ_{H} : 3.63 (s, 3H, $-\text{CO}_2\text{CH}_3$), 3.52 (s, 1H, CH-15), 2.46 (t, 2H, CH_2 -17), 1.17 (s, 3H, CH_3 -20), 0.84 (s, 3H, CH_3 -22), 2.29–0.83 (m, 21H). ^{13}C NMR (100 MHz, D_3COD) δ_{C} : 179.6 (2 \times C (O)2), 88.3, 76.0, 58.1, 56.3, 51.6, 48.5, 45.0, 43.0, 41.8, 40.8, 39.1, 37.1, 36.7, 29.1, 29.0, 28.0, 26.7, 22.3, 20.1, 19.6, 16.0.

Et_3B -mediated ATRA of iodoacetonitrile to 15 α -hydroxy-*ent*-kaurenoic acid

15 α -Hydroxy-*ent*-kaurenoic acid **18** (70 mg, 0.22 mmol) in 2.0 mL EtOH was treated under N_2 with iodoacetonitrile (32 μL , 0.44 mmol), PhSO_2N_3 (120 mg, 0.66 mmol), and Et_3B (0.88 mL, 0.88 mmol). The reaction mixture was purified by FC ($\text{CH}_2\text{Cl}_2/\text{MeOH}$ 95:5) and provided compound **25** (48 mg, 54%) as a colorless oil (contaminated with PhSO_2N_3).

Nitrile 25

Colorless oil. IR (ν , cm^{-1}): 3836, 3673, 2988, 2973, 2902, 2653, 1698, 1404, 1394, 1381, 1242. ^1H NMR (400 MHz, D_3COD) δ_{H} : 5.29 (s, 1H, OH), 2.71–2.81 (m, 2H, CH_2 -18), 2.54 (s, 1H, CH-15), 1.24 (s, 3H, CH_3 -20), 0.94 (s, 3H, CH_3 -22), 2.42–0.77 (m, 21H). ^{13}C NMR (100 MHz, D_3COD) δ_{H} : 183.9, 119.4, 85.5, 83.2, 56.4, 55.4, 53.4, 50.3, 47.5, 43.6, 40.5, 39.8, 38.8, 37.9, 37.6, 36.1, 28.8, 26.4, 20.8, 19.1, 18.8, 15.5.

Azidoester 26

To a stirred solution of azidoacid **24** (45 mg, 0.10 mmol) in approximately 5 mL of Et_2O at 0 $^\circ\text{C}$, an etheric solution of CH_2N_2 was added dropwise until the yellow color persisted (0.2–0.25 mmol). The mixture was stirred for 30 min and concentrated to give the crude product, which was purified by column chromatography (pentane/ EtOAc 95:5) to give azidoester **26** (41 mg, 99%) as a colorless oil.

Colorless oil. $[\alpha]_{\text{D}}^{20} = -55.8$ ($c = 2.13$, CHCl_3). IR (ν , cm^{-1}): 3737, 3526 (w), 2940, 2872, 2853, 2299, 2107, 1725, 1445. ^1H NMR (400 MHz, CDCl_3) δ_{H} : 3.69 (s, 3H, C-19 ($-\text{CO}_2\text{CH}_3$)), 3.63 (s, 3H, C-21, $-\text{CO}_2\text{CH}_3$), 3.40 (s, 1H, CH-15), 2.56 (t, $J = 7.9$ Hz, 2H, CH_2 -18), 1.16 (s, 3H, CH_3 -20), 0.81 (s, 3H, CH_3 -22), 2.16–0.78 (m, 21H). ^{13}C NMR (100 MHz, CDCl_3) δ_{C} : 177.84, 173.61, 85.22, 75.44, 56.71, 54.72, 51.71, 51.06, 47.55, 43.78, 41.87, 40.59, 39.59, 37.98, 36.05, 35.66, 29.41, 28.63, 28.41, 25.78, 21.03, 18.99, 18.19, 15.34.

Lactam 27

A solution of azidoester **26** (53 mg, 0.12 mmol) and 10% Pd/C (10% w/w) in dry EtOAc (2 mL) was stirred for 64 h at room temperature under H_2 (1 atm). The catalyst was filtered off, the solvent was removed under reduced pressure, and the crude purified by FC ($\text{CH}_2\text{Cl}_2/\text{MeOH}$ 85:15), giving lactam **27** (16 mg, 35%) as a yellowish oil.

Yellowish oil. $[\alpha]_{\text{D}}^{20} = -90.8$ ($c = 3.0$, CHCl_3). IR (ν , cm^{-1}): 3351, 2933, 2871, 2322, 1722, 1685, 1552. ^1H NMR (400 MHz, CDCl_3) δ_{H} : 6.73 (s, 1H, NH), 3.63 (s, 3H, $-\text{CO}_2\text{CH}_3$), 3.49 (s, 1H, CH-15), 2.44–2.27 (m, 2H), 1.16 (s, 3H, CH_3 -20), 0.81 (s, 3H, CH_3 -22), 2.14–0.79 (m, 21H). ^{13}C NMR (100 MHz, CDCl_3) δ_{C} : 179.1, 178.0, 88.2, 70.8, 56.8, 54.4, 51.1, 47.4, 44.9, 43.7, 40.7, 38.0, 39.6, 36.6, 35.4, 30.6, 29.3, 28.6, 26.3, 21.2, 19.1, 19.0, 15.5.

4. Conclusions

Modifications of *ent*-kaurenoic acid derivatives at the *exo*-methylenic double bond of the tetracyclic diterpenic framework based on mild radical mediated C–C bond forming reactions such as the iodine ATRA and the azidoalkylation reaction have been performed. Although this reaction has been demonstrated previously on other substrates, their application in complex natural compounds is not well documented and far from trivial due to the potential side reactions such as intramolecular hydrogen atom transfers. Both steric and electronic factors strongly influence the outcome of the free radical sequences, providing unprecedented avenues for expanding structural diversity of natural products.

The azidoalkylation reaction proved to be extremely useful in the context of increasing structural complexity of the parent natural scaffold, including simultaneous functional-

ization with different heteroatomic functional groups. The advantage of the tertiary azide moiety was demonstrated by subsequent reductions, leading to spiro-fused lactam and pyrrolidine fragments. The reported structural modifications led to a series of new compounds with relevant biological activity, which was demonstrated by in vitro cytotoxicity tests on several tumor cell lines. The hybrid terpene-nitrogen containing heterocycles with unprecedented spiro-junction have shown relevant cytotoxicity and promising selectivity indexes. These results represent a solid basis for following research on the synthesis of such derivatives based on available natural product templates.

Supplementary Materials: The following are available online. X-ray crystal structure report for lactam **12** (CCDC 2023783), X-ray crystal structure report for lactone **22** (CCDC 2023785), IR and NMR spectra of compounds **11**, **12**, **13**, **16**, **22**, **25**, **26**, **27**, IC₅₀, and SI data for investigated *ent*-kauranic derivatives.

Author Contributions: Conceptualization, supervision and funding acquisition, P.R. and V.K.; preparation of substrates and chemical synthesis, N.U., E.P. and V.G.; evaluation of cytotoxicity, L.P. and D.D.; writing—original draft preparation, V.K.; writing—review and editing, P.R. All authors have read and agreed to the published version of the manuscript.

Funding: This research was funded by the SCOPES program of the Swiss National Science Foundation, project IZ73Z0_152346/1; the Swiss National Science Foundation, projects 200020_172621 and 200020_201092; and the National Agency for Research and Development (ANCD) of the Republic of Moldova, grant number 20.80009.8007.03.

Institutional Review Board Statement: Not applicable.

Informed Consent Statement: Not applicable.

Data Availability Statement: Data of the compounds are available on request from the corresponding authors.

Acknowledgments: The X-ray crystal structure determination service unit of the Department of Chemistry, Biochemistry, and Pharmaceutical Sciences of the University of Bern (P. Macchi and J. Hauser) is acknowledged for measuring, solving, refining, and summarizing the structures of compounds **12** and **22**.

Conflicts of Interest: The authors declare no conflict of interest.

Sample Availability: Samples of the compounds are available on request from the corresponding authors.

References

1. Hanson, J.R.; Oliveira, B.H.D. Stevioside and Related Sweet Diterpenoid Glycosides. *Nat. Prod. Rep.* **1993**, *10*, 301–309. [[CrossRef](#)]
2. Ghisalberti, E.L. The Biological Activity of Naturally Occurring Kaurane Diterpenes. *Fitoterapia* **1997**, *68*, 303–325.
3. Kataev, E.; Khaybullin, R.N.; Sharipova, R.R.; Stroykina, I.Y. Ent-Kaurane Diterpenoids and Glycosides: Isolation, Properties, and Chemical Transformations. *Rev. J. Chem.* **2011**, *1*, 93–160. [[CrossRef](#)]
4. Villa-Ruano, N.; Lozoya-Gloria, E.; Pacheco-Hernández, Y. Kaurenoic Acid. In *Studies in Natural Products Chemistry*; Elsevier: Amsterdam, The Netherlands, 2016; Volume 51, pp. 151–174. ISBN 978-0-444-63932-5.
5. Wang, L.; Li, D.; Wang, C.; Zhang, Y.; Xu, J. Recent Progress in the Development of Natural Ent-Kaurane Diterpenoids with Anti-Tumor Activity. *Mini Rev. Med. Chem.* **2011**, *11*, 910–919. [[CrossRef](#)]
6. Hutt, O.E.; Doan, T.L.; Georg, G.I. Synthesis of Skeletally Diverse and Stereochemically Complex Library Templates Derived from Isosteviol and Steviol. *Org. Lett.* **2013**, *15*, 1602–1605. [[CrossRef](#)]
7. Lohelster, C.; Weckbecker, M.; Waldvogel, S.R. (–)-Isosteviol as a Versatile Ex-Chiral-Pool Building Block for Organic Chemistry: (–)-Isosteviol as a Building Block for Organic Chemistry. *Eur. J. Org. Chem.* **2013**, *2013*, 5539–5554. [[CrossRef](#)]
8. Peixoto, A.F.; de Melo, D.S.; Fernandes, T.F.; Fonseca, Y.; Gusevskaya, E.V.; Silva, A.M.S.; Contreras, R.R.; Reyes, M.; Usubillaga, A.; dos Santos, E.N.; et al. Rhodium Catalyzed Hydroformylation of Kaurane Derivatives: A Route to New Diterpenes with Potential Bioactivity. *Appl. Catal. Gen.* **2008**, *340*, 212–219. [[CrossRef](#)]
9. Hueso-Falcón, I.; Girón, N.; Velasco, P.; Amaro-Luis, J.M.; Ravelo, A.G.; de las Heras, B.; Hortelano, S.; Estevez-Braun, A. Synthesis and Induction of Apoptosis Signaling Pathway of Ent-Kaurane Derivatives. *Bioorg. Med. Chem.* **2010**, *18*, 1724–1735. [[CrossRef](#)] [[PubMed](#)]
10. Qiu, Y.; Gao, S. Trends in Applying C–H Oxidation to the Total Synthesis of Natural Products. *Nat. Prod. Rep.* **2016**, *33*, 562–581. [[CrossRef](#)] [[PubMed](#)]

11. Shugrue, C.R.; Miller, S.J. Applications of Nonenzymatic Catalysts to the Alteration of Natural Products. *Chem. Rev.* **2017**, *117*, 11894–11951. [[CrossRef](#)]
12. Stateman, L.; Nakafuku, K.; Nagib, D. Remote C–H Functionalization via Selective Hydrogen Atom Transfer. *Synthesis* **2018**, *50*, 1569–1586. [[CrossRef](#)]
13. Kharasch, M.S.; Jensen, E.V.; Urry, W.H. Addition of Carbon Tetrachloride and Chloroform to Olefins. *Science* **1945**, *102*, 128. [[CrossRef](#)]
14. Kharasch, M.S.; Urry, W.H.; Jensen, E.V. Addition of Derivatives of Chlorinated Acetic Acids to Olefins. *J. Am. Chem. Soc.* **1945**, *67*, 1626. [[CrossRef](#)]
15. Kharasch, M.S.; Skell, P.S.; Fisher, P. Reactions of Atoms and Free Radicals in Solution. XII. The Addition of Bromo Esters to Olefins. *J. Am. Chem. Soc.* **1948**, *70*, 1055–1059. [[CrossRef](#)]
16. Byers, Jeffrey Atom Transfer Reactions. In *Radicals in Organic Synthesis*; Renaud, P.; Sibi, M.P. (Eds.) Wiley-VCH Verlag GmbH: Weinheim, Germany, 2001; Volume 1, pp. 72–89. ISBN 3-527-301 60-7.
17. Pintauer, T.; Matyjaszewski, K. Atom Transfer Radical Addition and Polymerization Reactions Catalyzed by PPM Amounts of Copper Complexes. *Chem. Soc. Rev.* **2008**, *37*, 1087. [[CrossRef](#)] [[PubMed](#)]
18. Meyer, D.; Vin, E.; Wyler, B.; Lapointe, G.; Renaud, P. Facile Preparation of Functionalized 1-Substituted Cycloalkenes via an Iodine Atom Transfer Radical Addition–Elimination Process. *Synlett* **2016**, *27*, 745–748. [[CrossRef](#)]
19. Tappin, N.D.C.; Renaud, P. Methyl Radical Initiated Kharasch and Related Reactions. *Adv. Synth. Catal.* **2021**, *363*, 275–282. [[CrossRef](#)]
20. Renaud, P.; Ollivier, C.; Panchaud, P.; Panchaud, P. Radical Carboazidation of Alkenes: An Efficient Tool for the Preparation of Pyrrolidinone Derivatives. *Angew. Chem. Int. Ed. Engl.* **2002**, *41*, 3460–3462. [[CrossRef](#)]
21. Panchaud, P.; Chabaud, L.; Landais, Y.; Ollivier, C.; Renaud, P.; Zigmantas, S. Radical Amination with Sulfonyl Azides: A Powerful Method for the Formation of CN Bonds. *Chem. Eur. J.* **2004**, *10*, 3606–3614. [[CrossRef](#)]
22. Lapointe, G.; Kapat, A.; Weidner, K.; Renaud, P. Radical Azidation Reactions and Their Application in the Synthesis of Alkaloids. *Pure Appl. Chem* **2012**, *84*, 1633–1641. [[CrossRef](#)]
23. Panchaud, P.; Ollivier, C.; Renaud, P.; Zigmantas, S. Radical Carboazidation: Expedient Assembly of the Core Structure of Various Alkaloid Families. *J. Org. Chem.* **2004**, *69*, 2755–2759. [[CrossRef](#)] [[PubMed](#)]
24. Weidner, K.; Giroult, A.; Panchaud, P.; Renaud, P. Efficient Carboazidation of Alkenes Using a Radical Desulfonylative Azide Transfer Process. *J. Am. Chem. Soc.* **2010**, *132*, 17511–17515. [[CrossRef](#)]
25. Cren, S.; Schär, P.; Renaud, P.; Schenk, K. Diastereoselectivity Control of the Radical Carboazidation of Substituted Methylenecyclohexanes. *J. Org. Chem.* **2009**, *74*, 2942–2946. [[CrossRef](#)]
26. Torres, A.; Molinillo, J.M.G.; Varela, R.M.; Casas, L.; Mantell, C.; Martínez de la Ossa, E.J.; Macías, F.A. Helikaurolides A–D with a Diterpene–Sesquiterpene Skeleton from Supercritical Fluid Extracts of *Helianthus annuus* L. Var. Arianna. *Org. Lett.* **2015**, *17*, 4730–4733. [[CrossRef](#)] [[PubMed](#)]
27. Ollivier, C.; Bark, T.; Renaud, P. An Efficient and Practical Tin Free Procedure for Radical Iodine Atom-Transfer Reactions. *Synthesis* **2000**, *2000*, 1598–1602. [[CrossRef](#)]
28. Ollivier, C.; Renaud, P. A Novel Approach for the Formation of Carbon–Nitrogen Bonds: Azidation of Alkyl Radicals with Sulfonyl Azides. *J. Am. Chem. Soc.* **2001**, *123*, 4717–4727. [[CrossRef](#)] [[PubMed](#)]
29. Bräse, S.; Gil, C.; Knepper, K.; Zimmermann, V. Organic Azides: An Exploding Diversity of a Unique Class of Compounds. *Angew. Chem. Int. Ed.* **2005**, *44*, 5188–5240. [[CrossRef](#)]
30. Agalave, S.G.; Maujan, S.R.; Pore, V.S. Click Chemistry: 1,2,3-Triazoles as Pharmacophores. *Chem. Asian J.* **2011**, *6*, 2696–2718. [[CrossRef](#)]
31. Panchaud, P.; Renaud, P. A Convenient Tin-Free Procedure for Radical Carboazidation and Azidation. *J. Org. Chem.* **2004**, *69*, 3205–3207. [[CrossRef](#)]
32. Panchaud, P.; Renaud, P. Tin-Free Radical Carboazidation. *Chim. Int. J. Chem.* **2004**, *58*, 232–233. [[CrossRef](#)]
33. Brown, H.C.; Hebert, N.C. Organoboranes: XXXIII. Protonolysis of Triethylborane with Carboxylic Acids. *J. Organomet. Chem.* **1983**, *255*, 135–141. [[CrossRef](#)]
34. Suzuki, A. Organoboranes in Organic Syntheses Including Suzuki Coupling Reaction. *Heterocycles* **2010**, *80*, 15–43. [[CrossRef](#)]
35. Harish, V.; Periasamy, M. Enantiomerically Pure Piperazines via NaBH₄/I₂ Reduction of Cyclic Amides. *Tetrahedron Asymmetry* **2017**, *28*, 175–180. [[CrossRef](#)]
36. CCDC 2023783 and 2023785 Contain the Supplementary Crystallographic Data for Compound **12** and **22**. Available online: <http://www.Ccdc.Cam.Ac.Uk>. (accessed on 23 July 2021).
37. Curran, D.P.; Bosch, E.; Kaplan, J.; Newcomb, M. Rate Constants for Halogen Atom Transfer from Representative. Alpha.-Halo Carbonyl Compounds to Primary Alkyl Radicals. *J. Org. Chem.* **1989**, *54*, 1826–1831. [[CrossRef](#)]
38. Badisa, R.B.; Darling-Reed, S.F.; Joseph, P.; Cooperwood, J.S.; Latinwo, L.M.; Goodman, C.B. Selective Cytotoxic Activities of Two Novel Synthetic Drugs on Human Breast Carcinoma MCF-7 Cells. *Anticancer Res.* **2009**, *29*, 2993–2996.
39. Genomics of Drug Sensitivity in Cancer. Available online: <https://www.cancerrxgene.org> (accessed on 30 July 2020).
40. Saldívar-González, F.I.; Lenci, E.; Trabocchi, A.; Medina-Franco, J.L. Exploring the Chemical Space and the Bioactivity Profile of Lactams: A Chemoinformatic Study. *RSC Adv.* **2019**, *9*, 27105–27116. [[CrossRef](#)]

41. Caruano, J.; Muccioli, G.G.; Robiette, R. Biologically Active γ -Lactams: Synthesis and Natural Sources. *Org. Biomol. Chem.* **2016**, *14*, 10134–10156. [[CrossRef](#)]
42. *CrysAlisPro (Version 1.171.34.44)*; Oxford Diffraction Ltd.: Yarnton, UK, 2010.
43. Macchi, P.; Bürgi, H.-B.; Chimpri, A.S.; Hauser, J.; Gál, Z. Low-Energy Contamination of Mo Microsource X-Ray Radiation: Analysis and Solution of the Problem. *J. Appl. Crystallogr.* **2011**, *44*, 763–771. [[CrossRef](#)]
44. Sheldrick, G.M. *SHELXT*—Integrated Space-Group and Crystal-Structure Determination. *Acta Crystallogr. Sect. Found. Adv.* **2015**, *71*, 3–8. [[CrossRef](#)]
45. Sheldrick, G.M. Crystal Structure Refinement with *SHELXL*. *Acta Crystallogr. Sect. C Struct. Chem.* **2015**, *71*, 3–8. [[CrossRef](#)] [[PubMed](#)]
46. Dolomanov, O.V.; Bourhis, L.J.; Gildea, R.J.; Howard, J.A.K.; Puschmann, H. *OLEX2*: A Complete Structure Solution, Refinement and Analysis Program. *J. Appl. Crystallogr.* **2009**, *42*, 339–341. [[CrossRef](#)]